



Glacial geomorphology of the central Tibetan Plateau

BJÖRN MORÉN, JAKOB HEYMAN and ARJEN P. STROEVEN

Department of Physical Geography and Quaternary Geology, Stockholm University, SE-106 91 Stockholm, Sweden;
bjmo7547@student.su.se.

Abstract

The glacial geomorphology of the central Tibetan Plateau was mapped over 285,000 km². Here we present a map covering 135,000 km² at a scale of 1:660,000. The glacial geomorphology was mapped using 15 and 30 m resolution Landsat 7 ETM+ satellite imagery, a 90 m resolution SRTM digital elevation model, and satellite and aerial images displayed in Google Earth. Four landform categories were discernible and mapped; glacial valleys, marginal moraines, glacial lineations, and hummocky terrain. The mapped landforms indicate multiple glacial advances of valley and piedmont glaciers. The mapped landform record lends no support to individual ice centres having coalesced to form a plateau-wide ice sheet.



(Received 15th October 2010; Revised 14th January 2011; Accepted 17th January 2011)



1. Introduction

1.1 Geological outline

A number of plateau-wide glacial reconstructions exist for the Tibetan Plateau (e.g., Frenzel, 1960; Li et al., 1991; Shi et al., 1992; Kuhle, 2004; Lehmkuhl and Owen, 2005). However, landform evidence on which to base such reconstructions is often insufficiently documented. Glacial geomorphological maps have thus far mainly been produced for individual mountain areas and cover restricted regions of the Tibetan Plateau (e.g. Derbyshire et al., 1991; Zheng and Rutter, 1998; Shi et al., 2005). Heyman et al. (2008) presented the glacial geomorphology for a large section of the NE Tibetan Plateau, and glacial reconstructions inferred from this work (Heyman, 2010) reveal important discrepancies with previously presented plateau-wide reconstructions for this area (Heyman et al., 2009). In order to continue documenting evidence for former glaciations in Tibet, we present a glacial geomorphological map covering an extensive part of the central Tibetan Plateau.

The study area covers 850x335 km (285,000 km²) on the north-central Tibetan Plateau (Figure 1), from the glaciated Tanggula Shan (Shan = mountain) in the east, across the Puruogangri ice field, to the Zangsergangri ice field in the northwest, and has an average altitude of 4970 m a.s.l. Tanggula Shan is one of the most prominent mountain ranges on the Tibetan Plateau. It extends *ca.* 500 km in a NW-SE direction, with considerable contemporary glaciation, and with glaciers up to *ca.* 10 km long, centered around the highest peak (Geladandong, 6566 m a.s.l.). Glacial landform maps covering the highest parts of the Tanggula Shan have been presented by Zheng and Jiao (1991), Jiao and Shen (2005) and Colgan et al. (2006).

Attempts to determine the glacial history of the mapped area, primarily using cosmogenic exposure dating, come from Schäfer et al. (2002), Owen et al. (2005) and Colgan et al. (2006). They presented exposure ages from Tanggula Shan samples located 2-30 km distance from contemporary glacier margins that range from *ca.* 16 ka to 215 ka (*cf.* Figure 2 for sample locations). With all but one sample older than 30 ka, the dataset has been interpreted to indicate a highly restricted glacial extent during the global last glacial maximum (LGM). Yi et al. (2002) presented electron spin resonance dates from aeolian sands overlying a series of moraine ridges up to 11.5 km beyond the present Puruogangri ice-field margin with an oldest age occurring on the outermost moraine of *ca.* 53 ka, corroborating the restricted LGM interpretation.

With the “glacial geomorphology of the central Tibetan Plateau” map we cover an extensive area of the Tibetan Plateau and add another coherent account of the extent of former glaciation to a neighbouring region for which similarly-detailed glacial landform maps

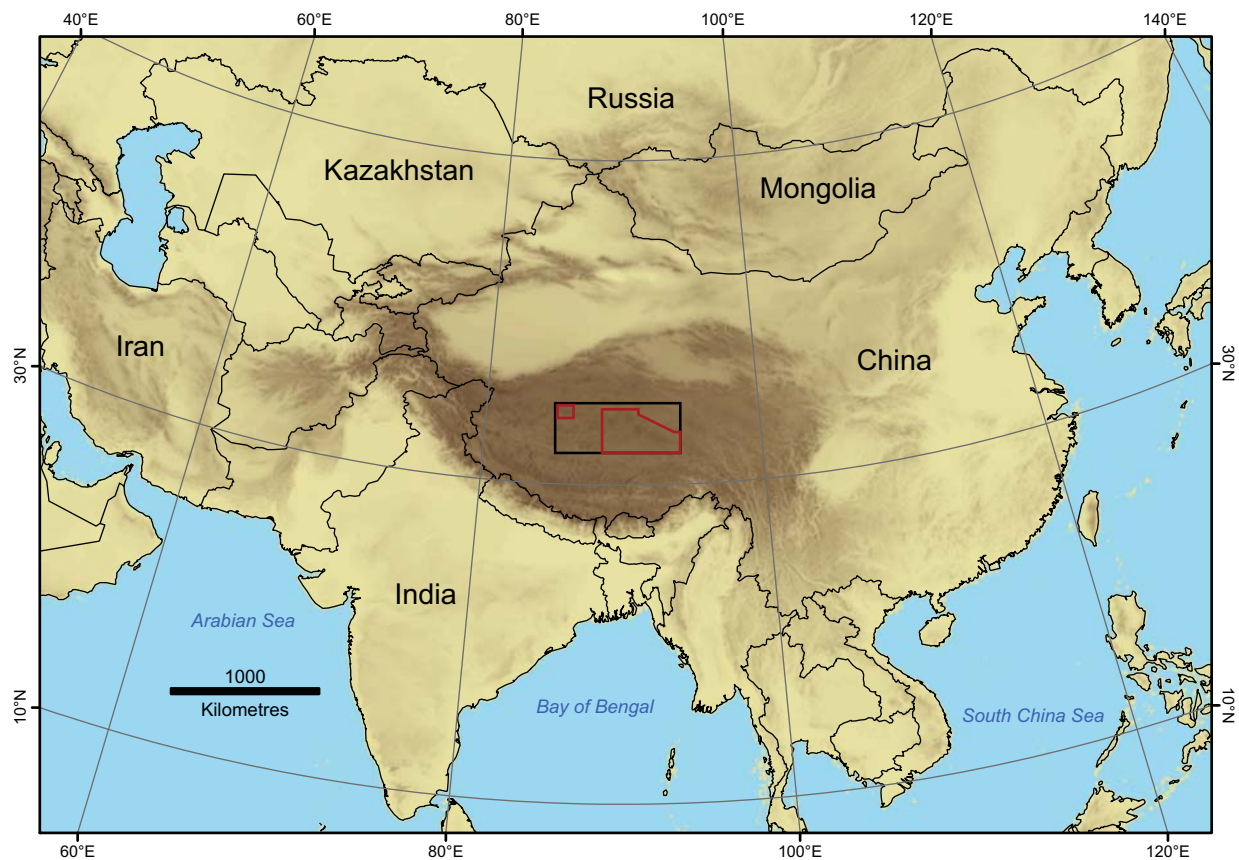


Figure 1. Overview of Asia with the black box showing the study area (285,000 km²) and the red boxes inside the black box showing the areas depicted on the large-scale map (135,000 km²).

have been produced (*cf.* Heyman et al., 2008; Stroeven et al., 2009). This landform record could usefully be used to underpin future (plateau-wide) glacial reconstructions.

2. Methods

The glacial geomorphology has been mapped from a shuttle radar topography mission (SRTM) digital elevation model (DEM; 90 m horizontal resolution; Jarvis et al., 2008), together with Landsat 7 ETM+ satellite imagery (Table 1; GLCF, 2009). The satellite images were compiled into false-colour composites of bands 5, 4, 2 (30 m resolution). A semi-transparent grey-scale image of the panchromatic band 8 (15 m resolution) was draped over the false-colour composites to improve spatial resolution. Contemporary glacier cover was acquired from the GLIMS project (Armstrong et al., 2005). All landforms were identified using various combinations of Landsat 7 ETM+ satellite imagery,

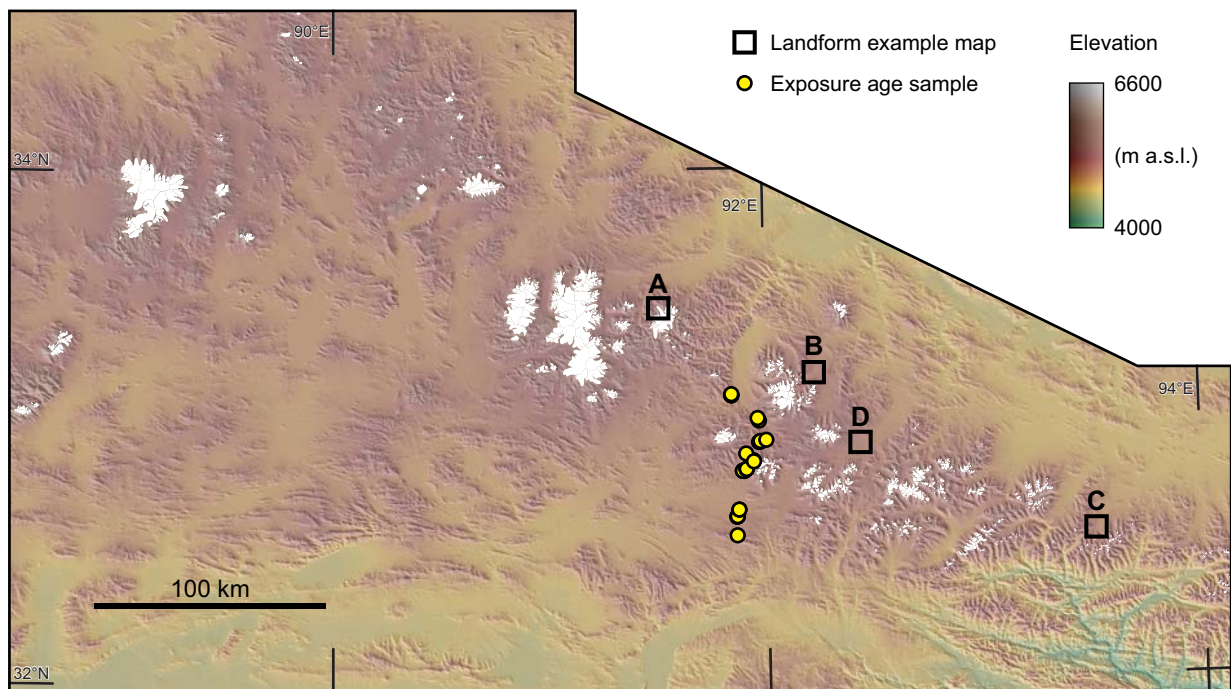


Figure 2. Map of the Tanggula Shan region of the study area (cf Figure 1 for location), with contemporary glaciers (white). A-D denote the location of landform examples shown in Figure 3. Cosmogenic exposure age locations are shown as yellow points (Schäfer et al., 2002; Owen et al., 2005; Colgan et al., 2006).

DEM, and Google Earth for 3D visualisation. The mapping was conducted at a scale of 1:100,000.

3. Landform descriptions

The landform definitions adopted here, and presented below, are based on the mapping of glacial morphology of the northeastern Tibetan Plateau (Heyman et al., 2008). The entire study area (black box in Figure 1) has been mapped. However, large areas lack discernible glacial landforms and some of these areas have therefore been omitted from the large-scale map. All parts of the study area were thoroughly searched for glacial landforms.

3.1 Glacial valleys

This category contains valleys with clear U-shaped cross-profiles and valleys with a trough-like shape (Figure 3A). Glacial valleys are located in the high mountain areas,

WRS Path	WRS Row	GLCF-ID	Acquisition date (y-m-d)
136	036	039-445	2000-08-31
137	036	039-244	2001-07-07
138	036	039-278	2001-10-03
139	036	039-079	2001-09-24
140	036	039-113	1999-08-25
141	036	039-155	1999-09-17
142	036	039-194	2002-05-27
136	037	039-446	1999-09-30
137	037	039-252	2001-07-08
138	037	039-279	2002-05-15
139	037	039-080	2000-10-07
140	037	039-114	1999-08-25
141	037	039-156	2001-09-22
142	037	039-195	2000-10-28
137	038	039-246	2000-12-28
138	038	039-280	2001-06-13
139	038	039-081	1999-09-19
140	038	039-115	2000-10-30
141	038	039-157	2001-09-22
142	038	039-196	2000-10-28

Table 1. Landsat 7 ETM+ images used for mapping the glacial geomorphology. All images are from [GLCF \(2009\)](#) (WRS: World Reference System).

presumably because glaciers formed on high ground and discharged outwards and downwards towards the surrounding plain and have primarily been identified using the DEM. Glacial valleys range from 1 to more than 40 km in length and from 0.6 to 8 km in width. The typical depth of the valleys is between 200 and 400 m.

3.2 Marginal moraines

Marginal moraines are deposited at the margin of a glacier and therefore mark the former position of its terminus. Marginal moraines in the study area are often located outside glacial valleys, formed along the margins of piedmont lobes, and typically are ridges with a gentle relief. Series of marginal moraines located at varying distances from their headwalls indicate multiple glacial stages. Marginal moraines have primarily been identified using the DEM and satellite imagery (Figure 3B). Typically, marginal moraines range in length between 1 and 6 km, with the longest moraine exceeding 22 km. They are up to 2.5 km wide and have a height of up to 150 m.

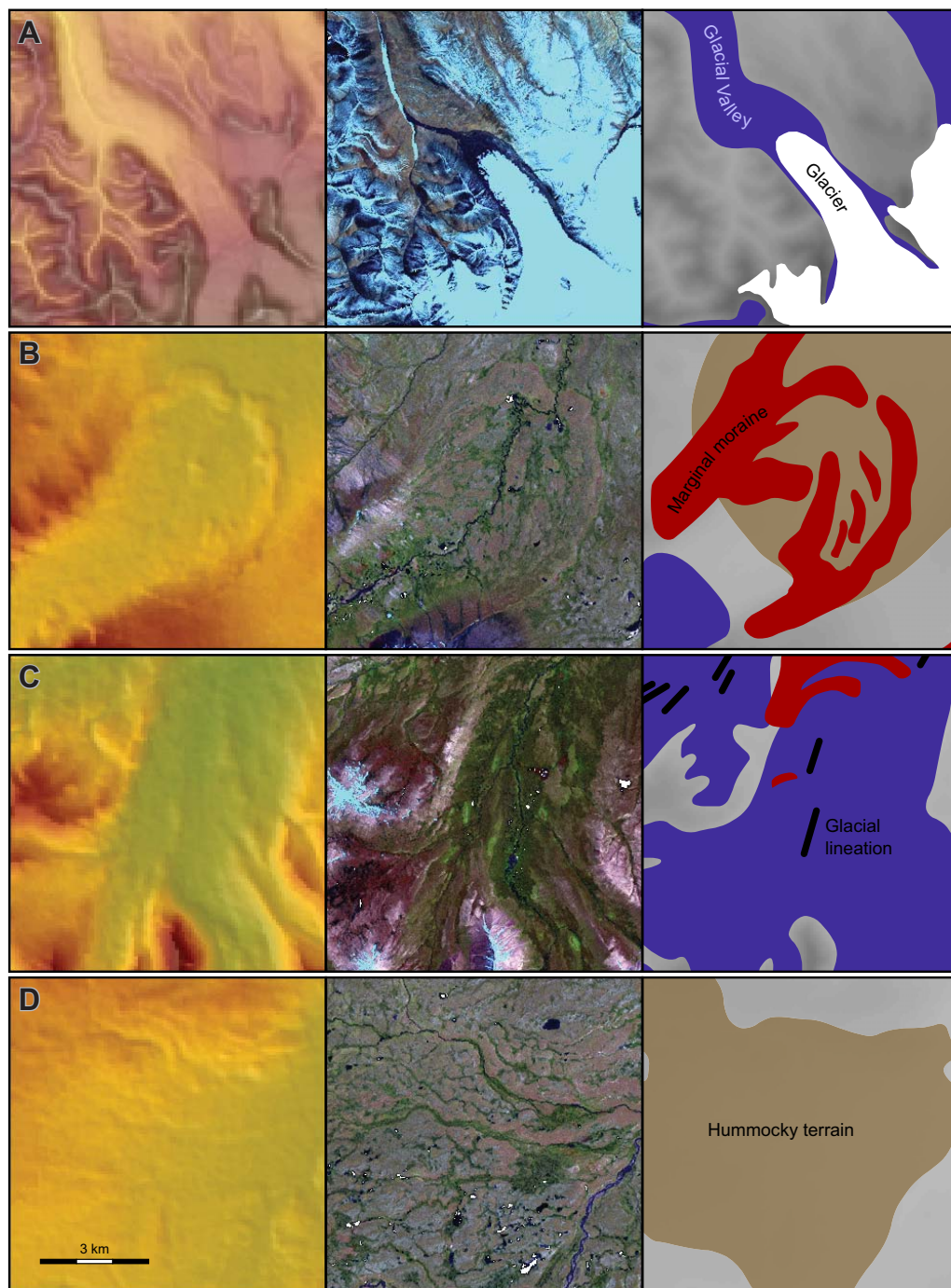


Figure 3. Landform category examples with SRTM DEM panels (left), Landsat 7 ETM+ satellite imagery (middle), and mapped landforms (right). All satellite images are colour composites of bands 5, 4, and 2, draped with a semi-transparent band 8. The DEM panels are draped by a semi-transparent slope image in panel A and by semi-transparent hillshade images in panels B, C, and D. North is towards the top of the maps and each map is 9x9 km. (A) Glacial valley in the upper left. Note the contemporary glacier in the lower right corner. (B) Marginal moraine deposited beyond the reaches of a glacial valley (lower left corner) and an integral part of the hummocky terrain area (*cf.* panel D). (C) Glacial lineations on the floor of glacial valleys. (D) Hummocky terrain area.

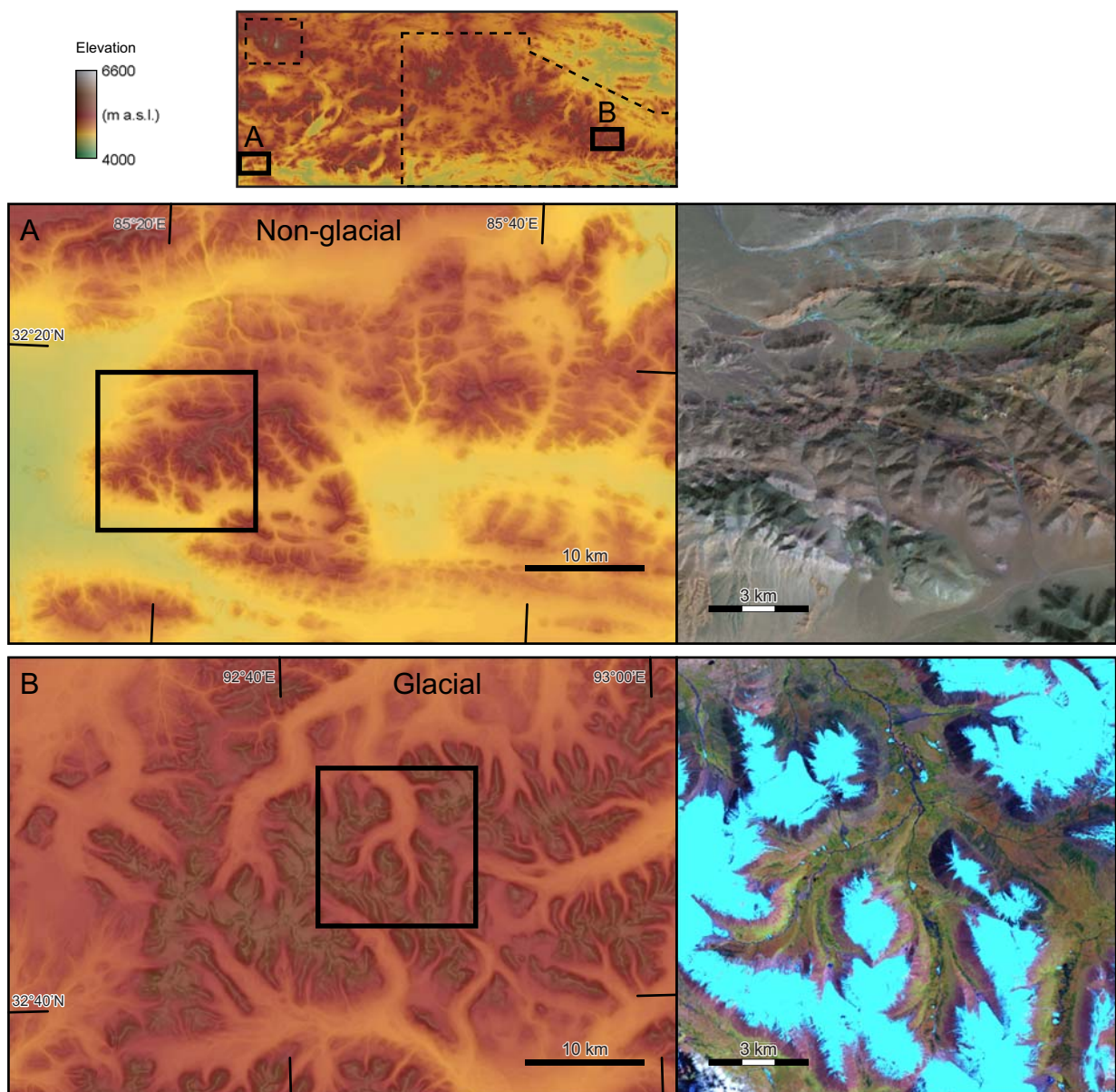


Figure 4. Comparison of a non-glacial (A) and a glacial (B) area using SRTM DEM draped with a semi-transparent slope image (left panels) and Landsat 7 ETM+ colour composites of bands 5, 4, and 2 (right panels). (A) The non-glacial area is characterised by a dense dendritic network of fluvially-carved V-shaped valleys and tectonic valleys. (B) The glacial area, on the other hand, is characterised by deeper and wider U-shaped valleys displaying a simpler dendritic pattern as glaciers successively deepened, widened and straightened their pre-existing fluvial valleys.

3.3 Glacial lineations

Glacial lineations are subglacially-formed elongated features that can consist entirely of sediment or bedrock, or exhibit a core of bedrock draped with sediments (e.g., crag-and-tails). Glacial lineations commonly occur in glacial valleys. DEM and satellite imagery

were the primary tools for identifying glacial lineations (Figure 3C). The typical length of glacial lineations is *ca.* 1 km, but lineations of more than 5 km occur.

3.4 Hummocky terrain

Hummocky terrain is a sedimentary deposit consisting of irregularly shaped mounds and depressions (Figure 3D; Eyles et al., 1999), considered here as a descriptive non-genetic term. This type of terrain typically has a gentle relief. A number of glacial processes might be involved in the formation of hummocky terrain (Benn and Evans, 2010). The most commonly inferred source of the material forming the hummocks is that of supraglacial debris being deposited in irregular hummocks during the uneven ablation of the ice it covers. Hummocky terrain mapped in this study and in Heyman et al. (2008) occurs close to glacial valleys and marginal moraines, corroborating a glacial genesis interpretation. Field studies of hummocky terrain on the NE margin of the Tibetan Plateau by Heyman et al. (2009) confirm their glacial origin. Because of its gentle relief, hummocky terrain has been identified almost entirely using satellite imagery and Google Earth. Hummocky terrain areas are irregular in plan-shape with the longest axis typically ranging between *ca.* 6 and 17 km (but up to more than 25 km). The diameter of individual mounds and depressions ranges from less than 0.1 km to more than 2 km.

4. Conclusions

The mapped glacial landforms help in an understanding of the central Tibetan Plateau palaeoglaciology. The landforms record the former existence of extended valley and piedmont glaciers in the high mountain areas. However, 87% of the surrounding plateau surface (248,000 km²) completely lacks discernible glacial landforms (*cf.* Figure 4), indicating a limited influence of glaciers on landscape development. Although glacial sediments and glacial landforms too small to be identified with the employed remote sensing techniques might exist in areas beyond those mapped as having glacial landforms in this study (*cf.* Heyman et al., 2009), the vastness of the areas lacking glacial landforms indicates former glaciations were restricted to the high mountain areas. The furthest distribution of glacial landforms in this study denotes the minimum extent of the maximum glaciation (Figure 5) with a total ice-covered area of at least 37,000 km² (13% of the study area). However, the timing of maximum glaciation in this large region may be non-synchronous for different areas, for which some caution is needed when considering the total ice-covered area. Landform assemblages commonly associated with ice-sheet scale glaciations, such as ribbed moraines, eskers, and drumlin swarms, are lacking. The mapped glacial landforms in a vast region of the central Tibetan Pla-

teau reveal evidence in support of mountain based glaciations but lend no support to the hypothesis of a Tibetan ice sheet.

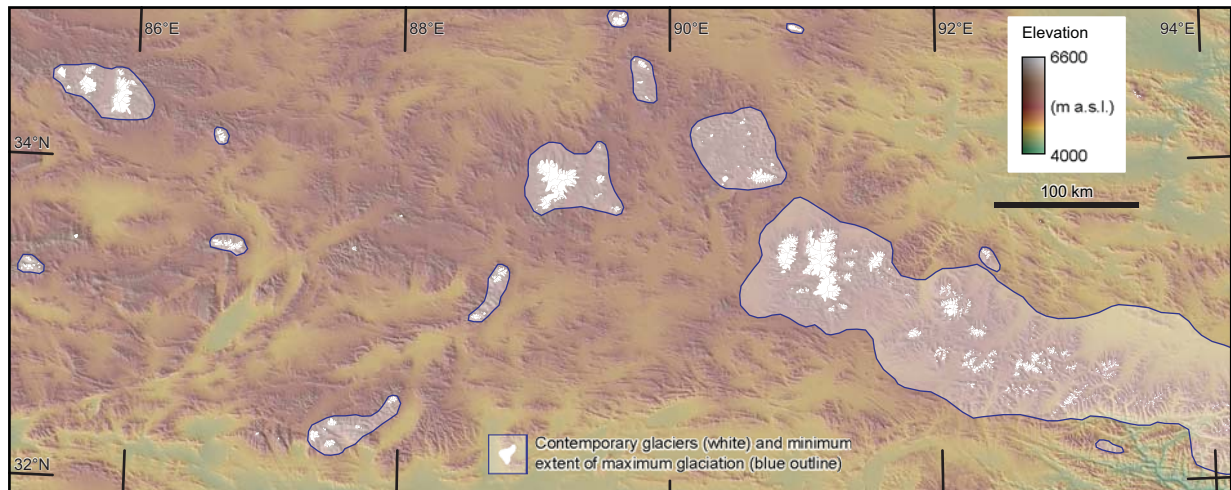


Figure 5. Minimum extent of maximum glaciation, based on mapped glacial landforms, covers 13% of the investigated area or 37,000 km². Glaciers may have reached their maximum extent at different times in the past

Software

The satellite images were processed into false-colour composites in ENVI 4.3. These composites, together with the DEM, were imported into ArcGIS 9.2, in which the mapping was performed. Google Earth was used to visualise the area in a 3D environment. Adobe Illustrator CS3/CS4 was used to produce the final layout of the map.

Data

The author has supplied data (as an ESRI Shapefile) used in the production of the accompanying map. This PDF has a ZIP archive embedded within it (stored as a .ZI file extension) containing the data and can be accessed by right-clicking on the “paperclip” icon at the beginning of this section (you will need to save the file and edit the file extension to .ZIP). Whilst the contents of the ZIP file are the sole responsibility of the author, the journal has screened them for appropriateness.

Acknowledgements

We thank Professors Chris D. Clark, Lewis A. Owen and Yi Chaolu for constructive comments that helped clarify the article. We also thank Dr. Corné P. J. M. van Elzaker for the cartographic review.

References

- ARMSTRONG, R., RAUP, B., KHALSA, S. J. S., BARRY, R., KARGEL, J., HELM, C. and KIEFFER, H. (2005) GLIMS glacier database [Online]. Available from: <http://www.glims.org>, [Last accessed: 5 August, 2009].
- BENN, D. I. and EVANS, D. J. A. (2010) *Glaciers and glaciation*, Hodder Education, 734 pp.
- COLGAN, P. M., MUNROE, J. S. and ZHOU, S. (2006) Cosmogenic radionuclide evidence for the limited extent of last glacial maximum glaciers in the Tanggula Shan of the central Tibetan Plateau, *Quaternary Research*, 65, 336–339, doi: [10.1016/j.yqres.2005.08.026](https://doi.org/10.1016/j.yqres.2005.08.026).
- DERBYSHIRE, E., SHI, Y., LI, J., ZHENG, B., LI, S. and WANG, J. (1991) Quaternary glaciation of Tibet: the geological evidence, *Quaternary Science Reviews*, 10, 485–510, doi: [10.1016/0277-3791\(91\)90042-S](https://doi.org/10.1016/0277-3791(91)90042-S).
- EYLES, N., BOYCE, J. J. and BARENDREGT, R. W. (1999) Hummocky moraine: sedimentary record of stagnant Laurentide Ice Sheet lobes resting on soft beds, *Sedimentary Geology*, 123, 163–174, doi: [10.1016/S0037-0738\(98\)00129-8](https://doi.org/10.1016/S0037-0738(98)00129-8).
- FRENZEL, B. (1960) *Die Vegetations- und Landschaftszonen Nord-Eurasiens während der Letzen Eiszeit und während der postglazialen Wärmezeit*, Unpublished PhD Thesis, Akademie der Wissenschaften und der Literatur, Wiesbaden.
- GLCF (2009) Global Land Cover Facility [Online]. Available from: <http://www.landcover.org>, [Last accessed: 10 August, 2009].
- HEYMAN, J. (2010) *Palaeoglaciology of the northeastern Tibetan Plateau*, Unpublished PhD Thesis, Department of Physical Geography and Quaternary Geology, Stockholm University.
- HEYMAN, J., HÄTTESTRAND, C. and STROEVEN, A. P. (2008) Glacial geomorphology of the Bayan Har sector of the NE Tibetan Plateau, *Journal of Maps*, v2008, 42–62, doi: [10.4113/jom.2008.96](https://doi.org/10.4113/jom.2008.96).
- HEYMAN, J., STROEVEN, A. P., ALEXANDERSON, H., HÄTTESTRAND, C., HARBOR, J., LI, Y. K., CAFFEE, M. W., ZHOU, L. P., VERES, D., LIU, F. and MACHIEDO, M. (2009) Palaeoglaciology of Bayan Har Shan, northeastern Tibetan Plateau: glacial geology indicates maximum extents limited to ice cap and ice field scales, *Journal of Quaternary Science*, 24, 710–727, doi: [10.1002/jqs.1305](https://doi.org/10.1002/jqs.1305).
- JARVIS, A., REUTER, H. I., NELSON, A. and GUEVARA, E. (2008) Hole-filled seamless SRTM data V4 [Online]. Available from: <http://srtm.csi.cgiar.org/>, [Last accessed: 5 August, 2009].
- JIAO, K. and SHEN, Y. (2005) Quaternary glaciations in the Tanggula Range, In SHI, Y., CUI, Z. and SU, Z., (eds.) *The Quaternary Glaciations and Environmental Variations in China*, Hebei Science and Technology Publishing House, pp. 309–325.

- KUHLE, M. (2004) The High Glacial (Last Ice Age and LGM) ice cover in High and Central Asia, In EHLERS, J. and GIBBARD, P. L., (eds.) *Quaternary Glaciations - Extent and Chronology, Part III*, Elsevier, pp. 175–199.
- LEHMKUHL, F. and OWEN, L. A. (2005) Late Quaternary glaciation of Tibet and the bordering mountains: a review, *Boreas*, 34, 87–100, doi: [10.1080/03009480510012908](https://doi.org/10.1080/03009480510012908).
- LI, B., LI, J., CUI, Z., ZHENG, B., ZHANG, Q., WANG, F., ZHOU, S., SHI, Z., JIAO, K. and KANG, J. (1991) Quaternary glacial distribution map of Qinghai-Xizang (Tibet) plateau, Map Scale 1:3,000,000.
- OWEN, L. A., FINKEL, R. C., BARNARD, P. L., MA, H. Z., ASAHI, K., CAFFEE, M. W. and DERBYSHIRE, E. (2005) Climatic and topographic controls on the style and timing of Late Quaternary glaciation throughout Tibet and the Himalaya defined by ^{10}Be cosmogenic radionuclide surface exposure dating, *Quaternary Science Reviews*, 24, 1391–1411, doi: [10.1016/j.quascirev.2004.10.014](https://doi.org/10.1016/j.quascirev.2004.10.014).
- SCHÄFER, J. M., TSCHUDI, S., ZHAO, Z., WU, X., IVY-OCCHS, S., WIELER, R., BAUR, H., KUBIK, P. W. and SCHLÜCHTER, C. (2002) The limited influence of glaciations on global climate over the past 170 000 yr, *Earth and Planetary Science Letters*, 194, 287–297, doi: [10.1016/S0012-821X\(01\)00573-8](https://doi.org/10.1016/S0012-821X(01)00573-8).
- SHI, Y. F., CUI, Z. J. and SU, Z. (2005) *The Quaternary glaciations and environmental variations in China*, Hebei Science and Technology Publishing House.
- SHI, Y. F., ZHENG, B. X. and LI, S. J. (1992) Last glaciation and maximum glaciation in the Qinghai-Xizang (Tibet) Plateau: A controversy to M. Kuhle's ice sheet hypothesis, *Zeitschrift für Geomorphologie NF Supplementband*, 84, 19–35.
- STROEVEN, A. P., HILTTESTRAND, C., HEYMAN, J., HARBOR, J., LI, Y. K., ZHOU, L. P., CAFFEE, M. W., ALEXANDERSON, H., KLEMAN, J., MA, H. Z. and LIU, G. N. (2009) Landscape analysis of the Huang He headwaters, NE Tibetan Plateau – Patterns of glacial and fluvial erosion, *Geomorphology*, 103, 212–226, doi: [10.1016/j.geomorph.2008.04.024](https://doi.org/10.1016/j.geomorph.2008.04.024).
- YI, C., LI, X. and QU, J. (2002) Quaternary glaciation of Puruogangri—the largest modern ice field in Tibet, *Quaternary International*, 97/98, 111–121, doi: [doi:10.1016/S1040-6182\(02\)00056-3](https://doi.org/10.1016/S1040-6182(02)00056-3).
- ZHENG, B. and JIAO, K. (1991) Quaternary glaciations and periglaciations in the Qinghai-Xizang (Tibetan) Plateau. Excursion guidebook XI, INQUA 1991, XIII International Congress, 54 pp.
- ZHENG, B. and RUTTER, N. (1998) On the problem of Quaternary glaciations, and the extent and patterns of Pleistocene ice cover in the Qinghai-Xizang (Tibet) Plateau, *Quaternary International*, 45/46, 109–122, doi: [10.1016/S1040-6182\(97\)00009-8](https://doi.org/10.1016/S1040-6182(97)00009-8).